www.dergipark.gov.tr
ISSN:2148-3736

El-Cezerî Journal of Science and Engineering
Vol: 10, No: 3, 2023 (492-505)
DOI: 10.31202/ecjse.1247180

ECJSE

Research Paper

Optimization of Monopole Consecutive Square-Shaped Patch Antenna with ANN for Wireless Communication Systems

Sena Esen Bayer KESKIN[1,a], Cem GÜLER[2,b], Batuhan USLU[3,c]

[1,3]Department of Electrical and Electronics Engineering, Kırklareli University, Kırklareli, Turkey
[2] Department of Lüleburgaz Faculty of Aeronautics and Astronautics, Kırklareli University, Kırklareli, Turkey
senakeskin@klu.edu.tr

Received: 03.02.2023 **Accepted:** 19.08.2023

Abstract: In recent years, Artificial Neural Network (ANN) applications in antenna structures have gained significant traction due to their potential to reduce design and calculation times, offering optimization and prediction capabilities. This study introduces a novel monopole patch antenna design featuring a consecutive square-shaped broadband microstrip-line-fed antenna. The proposed antenna exhibits an impressive impedance bandwidth of 68% (1.55 - 2.82 GHz), a remarkable return loss of -47.25 dB, and a directivity gain of 2.77 dBi. Simulation studies were conducted using CST™ Studio Suite electromagnetic simulation software. The ANN model developed based on feed-forward backpropagation demonstrates exceptional agreement with the simulation results, showcasing an accuracy of 99.61805% and performing 2769.231 times faster. With advancing technology, ANNs present an effective solution for addressing complex antenna design challenges arising from escalating data rate requirements and uninterrupted data transmission. These results open promising avenues for further advancements in antenna design aided by ANN applications.

Keywords: Artificial Neural Network, Feed-Forward Backpropagation, Monopole Patch Antenna, Wireless Communication Systems, Bandwidth

1. Introduction

The number of mobile device users is increasing daily, which leads to increased data traffic. As a result, different mobile standards are offered for data transfer to solve the increase in data traffic. DCS (1.71-1.88 GHz), digital cellular system in Europe, PCS (1.85-1.99 GHz), UMTS (1.92-2.17 GHz), LTE2300 (2300-2400MHz), LTE2500 (2500) personal communications service in the United States - 2690MHz) and ISM (2.40-2.485 GHz) different frequency bands are used [1]. Antennas used in wireless communication, which occurs in various frequency bands according to IEEE standards, should be able to operate in more than one standard, have wide bandwidth and a simple structure, compact size, and easy integration into RF circuits. Therefore, such an antenna can be used simultaneously in different frequency bands for different mobile services, such as loop antennas [2], planar inverted-F antennas (PIFAs) [3], bow-tie antennas [4], and monopole patch antennas. Monopole patch antennas have become the most preferred antenna type in recent years due to their many advantages, such as lightness, durability, suitability for fabrication in large quantities, and low cost. The main disadvantages of monopole patch antennas are their narrow bandwidth and low efficiency as a result of various losses. Various methods are used in the literature to increase bandwidth. The easiest of these methods is based on various configurations of patch geometry. Apart from basic geometric shapes, patch designs with E-shaped, pentagon-shaped, rectangular-shaped, and fractal geometries [5-9]. Another method of increasing the bandwidth is to make slots of various shapes on the beaming patch or ground plane [10-13]. Frequency selective surface usage [14,15], EBG structure usage [16,17], parasitic element usage [18,19], thick dielectric layer usage [20], short

How to cite this article
S.E. Bayer Keskin, C. Güler, and B. Uslu, "Optimization of Monopole Consecutive Square-Shaped Patch Antenna with ANN for Wireless Communication Systems," *El-Cezerî Journal of Science and Engineering*, vol. 10, no. 1, pp. 492-505, 2023.
ORCID: [a]0000-0001-8309-3393; [b]0000-0002-6631-7559; [c]0000-0002-2064-7843

circuit pin usage [21], stacked patch usage [22], usage metamaterial [23,24] all of these are used to increase bandwidth. However, it has cost-increasing and complex processing sequences in issues such as prototyping and fabrication.

A planar antenna suitable for integration into wireless devices capable of operating in more than one frequency band is offered by Lizzi et al. A single RF port powers the antenna without any matching circuit. It is designed to be operated in GSM and UMTS frequency bands [25]. In another study, an antenna designed to cover the UMTS, and ISM bands (1.92-2.48 GHz) is being manufactured and tested. The patch with a V-shaped slot is formed on an FR-4 substrate with dimensions of 100×100 mm2. The measured results report that the impedance bandwidth of 10 dB is more than 25% [26]. For wireless applications, a single-pole antenna operating on multiple bands is offered. The antenna consists of a crescent-shaped patch, a microstrip supply line, and a defected ground structure. This antenna has an impedance bandwidth of 58.3% (over 1.7–3.1 GHz) and an average gain of 1.75 dBi [27]. An innovative broadband planar antenna for mobile communications is presented in another study. The measurement results of the manufactured antenna have a bandwidth of 34.1% between frequencies of 1.7-2.4 GHz in the GSM/PCS/UMTS bands. Moreover, the proposed antenna has a peak gain of 3.4-4.2 dBi over the entire available bandwidth with a radiation efficiency of more than 81% [28]. Although many studies in the literature on DCS, PCS, and UMTS bands together, there is no antenna covering IEEE 802.11 b/g/n ISM bands. Table 1. shows the comparison of patch antennas in the literature to the antenna proposed in this study.

Table 1. Comparison of studies in the literature and proposed antenna.

Study	Dimension (mm)	Operation Frequency (GHz)	Bandwidth (≤10dB)
[8]	75.85×57.23×1.59 mm^3	2.39-2.45 GHz	60 MHz
[12]	138×90×0.8 mm^3	2.3-2.53 GHz	230 MHz
[24]	100×100×0.6 mm^3	1.92-2.48 GHz	560 MHz
[28]	45×35×10.5 mm^3	2.354-2.894 GHz	540 MHz
This Work	**65×80×1.6 mm^3**	**1.55-2.82 GHz**	**1.27 GHz**

Artificial Neural Network (ANN) applications in the literature have been widely preferred in patch antenna structures to reduce design and calculation times with optimization and prediction applications. With ANN applications, consistent relationships can be established between multiple nonlinear datasets in antenna studies [29-32]. Aneesh et al. designed an S-shaped rectangular monopole patch antenna (RMSA) for ISM-band applications in 2019 [29]. The simulation data of the designed antenna is compared using Quasi-Newton (QN), Broyden–Fletcher–Goldfarb–Shanno (BFGS), Bayesian Regulation (BR), Powell-Beale Conjugate Gradient (CGB), Conjugate Gradient with Fletcher-Peeves (CGF), Levenberg-Marquardt (LM) algorithm, One Step Secant (OSS), and Scaled Conjugate Gradient (SCG) algorithms. As a result of the testing and training stages, Levenberg-Marquardt (LM) algorithm is the most efficient algorithm in terms of analysis speed and accuracy ratio. In addition, an S-shaped rectangular monopole patch antenna operating at a center frequency of 2.62 GHz was physically manufactured to verify the study and obtain results that are compatible with the results of the ANN. In another study, Badra et al. studied the monopole patch antenna structure based on the combination of three elliptical geometries with three different radius values [30]. Dimension parameters of the three elliptical geometries were used as input data. Return loss and gain values were trained using ANN with Levenberg-Marquardt (LM) algorithm and compared with the simulation data. The designed monopole antenna operates in the 2.009-2.781 GHz band. In metamaterial structures, Sagik et al. observed the minimum error rate of 0.017716 MAE in

2021 using the Levenberg-Marquardt (LM) algorithm of ANN for gain and directivity optimization [31]. Furthermore, in 2020, they designed a C-shaped split ring resonator-type metamaterial antenna to determine the frequency, reflection coefficient values, and design parameters using the CST 3D Electromagnetic analysis software program. As a result of training simulation data using ANN, the percentage of predicting the data was calculated as 99.552%. In 2014, Kayabasi et al. conducted a study comparing Neuro-Fuzzy Inference System (ANFIS) and ANN resonant frequency estimation efficiencies in L-shaped compact monopole patch antenna structure. According to the results obtained during the test phase, error rate values of 0.454% for ANFIS and 0.537% for ANN were obtained [32]. Yang et al. proposed a novel approach, MSCNN-LSTM, to predict the return loss of UHF antennas in dual-band RFID tags. The model consists of three branches of MSCNN and LSTM, enabling the extraction of fine-grain localized information and overall features from the antenna. Experimental results show that MSCNN-LSTM outperforms other methods with lower mean absolute error (0.0073), mean square error (0.00032), and root mean square error (0.01814). Moreover, the prediction time is significantly reduced, taking only 0.927519 seconds for 100 UHF antennas, compared to 4800 seconds with HFSS. The designed dual-band RFID tag antenna meets the desired return loss values, demonstrating the effectiveness of the proposed approach for efficient antenna design in HF-UHF RFID applications [33]. Karanam and Kakkar proposed a microstrip patch antenna for vehicular communication applications within the 5G frequency band. The backpropagation algorithm was applied to optimize the antenna's dimensions, resulting in a 16% reduction compared to conventional approaches. A fractal geometry is applied to the patch, and the ground is recessed as a defected ground structure [34]. Khafaga et al. compare the performance of the proposed approach with traditional models such as multilayer perceptron (ML), K-nearest neighbors (K-NN), and basic LSTM. Evaluation criteria, including root mean square error (RMSE), mean absolute error (MAE), and mean bias error (MBE), are utilized to assess the effectiveness of the models. Experimental results demonstrate that the proposed approach achieves an RMSE of 0.003018, MAE of 0.001871, and MBE of 0.000205, which are superior to the values obtained from the other competing models [35].

In this study, a monopole patch antenna with a line feed consisting of consecutively placed square structures is designed as well as the gain, directivity, bandwidth, and resonant frequency values are modeled with ANN to provide high bandwidth and high return loss values and work on all various mobile communication frequencies such as DCS, PCS, UMTS, LTE2300, LTE2500, and ISM. Also, this study introduces an original antenna design and investigates the impact of employing Artificial Neural Networks (ANNs), particularly in the context of patch antenna designs, to expedite the antenna design process. The ANN model is utilized to ascertain crucial performance parameters of the antenna, including gain, directivity, bandwidth, and resonant frequency. This innovative approach offers a more efficient and effective antenna design process compared to conventional methods. The research findings conclusively demonstrate that the utilization of the ANN-based method enables a swifter generation of antenna designs customized for various mobile communication frequencies. As a result, this study represents a significant stride towards enhancing antenna design processes for modern communication systems. Section 1 presents a literature review of why antennas covering different mobile standards are essential and how ANN applications find a place in antenna design. Section 2.1 shows the design stages of the prototyped antenna, the dimension values of the antenna, and the reflection coefficient values (S_{11}). In section 2.2, the gain, directivity gain, bandwidth, and resonant frequency parameters are obtained from 144 proposed monopole patch antennas. They are used for the feed-forward backpropagation neural network for 100 antennas for education, 22 antennas for testing, and 22 antennas for the validation phase to determine the optimum ANN architecture for the adaptation of the output values listed in this section. Section 3.1, the 2D-3D gain curves of the proposed antenna and the surface current distribution results. Section 3.2 discusses the results obtained with the design program and ANNs in terms of error rate, efficiency, and operation time. In the last section, the simulation and ANN prediction results of the study are presented. This study provides a precious reference for the fast and accurate realization of monopole patch antenna designs suitable for use in multiple cellular standards by using ANN.

2. Experimental Methods

2.1. Antenna Design

The designed antenna operates DCS (1.71-1.88 GHz), PCS (1.85-1.99 GHz), UMTS (1.92-2.17 GHz) LTE 2300 (Band-40) 2300-2400, and ISM (IEEE 802.11 b/g/n) 2400-2495 bands. For this purpose, FR-4 material with a relative dielectric constant of 4.3 and loss tangent of 0.019≈0.02 is used as the substrate material. The thickness of the dielectric material is 1.6 mm. A 2-stage design is carried out until it reaches the proposed antenna. The first structure in Fig. 1a, Antenna I, is a square-shaped patch fed by a microstrip line and a partial ground plane. Its bandwidth varies between 2.08 GHz and 2.62 GHz. Thus the antenna design is revised to increase return loss and bandwidth values. The second structure given in Fig. 1b is the proposed antenna. It is designed by removing the square gaps from the second antenna for the aimed bandwidth and is named a consecutive square-shaped monopole patch antenna. The bandwidth is 1.27 GHz (1.55 GHz-2.82 GHz), and the proposed antenna's return loss is -47 dB. A comparison of the return loss (S_{11}) values of Antenna I and Proposed Antenna is given in Fig. 2. Dimensions of the proposed antenna are given in Table 2.

Table 2. Dimensions of the antenna proposed.

Parameter	D_W	D_L	F_L	G_L	a	h
Dimension (mm)	65	80	12	11.7	4.5	1.6

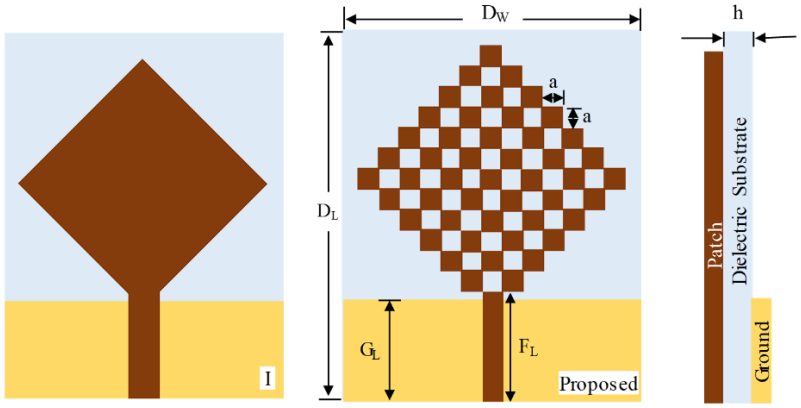

a) b)

Figure 1. The design evolution of the proposed antenna, (a) geometry of a rectangular printed monopole patch antenna - Antenna I, (b) geometry of consecutive square shaped monopole patch antenna - Proposed Antenna.

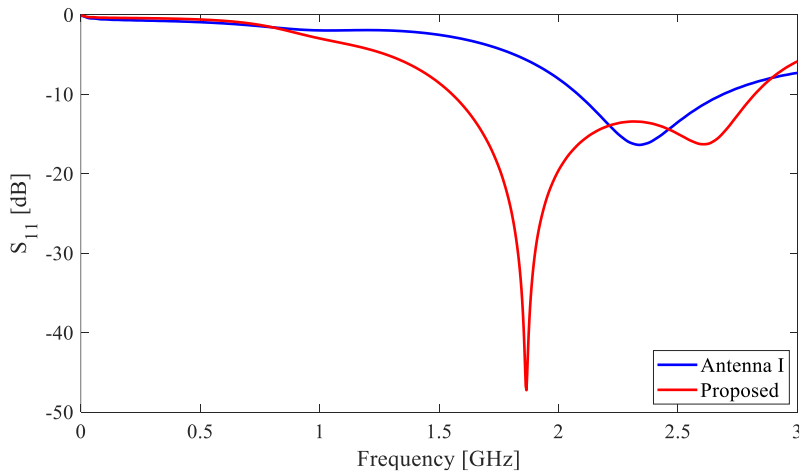

Figure 2. Comparison of the return loss (S_{11}) values of Antenna I and Proposed Antenna.

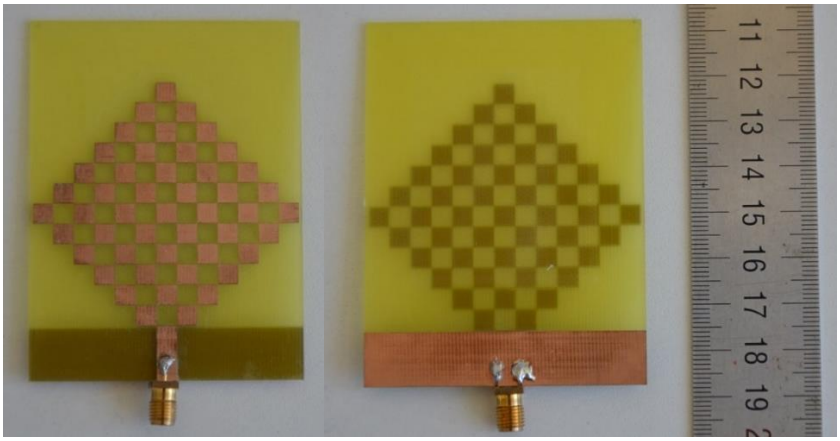

Figure 3. The fabrication structure of the proposed antenna (a) front view of Proposed Antenna (b) back view of Proposed Antenna.

The proposed antenna is fabricated using the LKPF ProtoMat S63 milling machine and measured using the Keysight E5063A Network Analyzer. The fabricated antenna is given in Fig. 3.

2.2. Neural Network Applications

This study aims for the proposed sequential square-shaped monopole antenna to operate in multiple frequency bands. For this purpose, computer-aided simulations of various electrical and dimensional parameters are performed for the proposed antenna. It is aimed to find the optimal parameters for the proposed antenna by analyzing the obtained simulation data as training samples through ANN. The electrical and dimensional parameters of the proposed antenna are given in Table 3. Here, (h) is the thickness of the dielectric material, (D_L) is the length of the antenna, (D_W) is the width of the antenna, (a) is the square size coefficient of the patch, and (ε_r) is the relative permittivity of dielectric material. These parameters are input parameters, and gain, directivity, resonant frequency, and bandwidth data are the output data of the ANN. In addition, 144 antenna simulations were performed for the ANN training performed for the proposed antenna. The dimension parameters are trained and tested with MATLAB™ Numerical Calculation Software and simulation data obtained from CST™ Microwave and Electromagnetic analysis software program.

Table 3. Physical and electrical parameters of simulated Consecutive Square-Shaped Microstrip Antennas.

Patch Dimensions					Number of Total Simulations
D_L	D_W	h	a	ε_r	144
65, 70, 75, 80	75, 80, 85	0.787, 1.575	4, 4.5, 5	2.2, 4.3	

The values obtained from the simulation are compared with the ANN for the training stages performed with MATLAB™ “nntool” on optimal ANN structures. The difference between the two values is defined as a numerical error.

In this study, Mean Squared Error (MSE) was used to decipher the difference between ANN and Simulation data. Fig. 4. shows that the error decision between the training results and the simulation results is calculated using the mean square error (MSE) method.

The fact that the training of the created ANN model takes place, and the consistency of the training is also tested with test data allows us to determine whether the model is available. The training

parameters are defined according to Table 4. and Table 6. The antenna data distributed for use during the training phase is defined by ANN according to the parameters in Table 5.

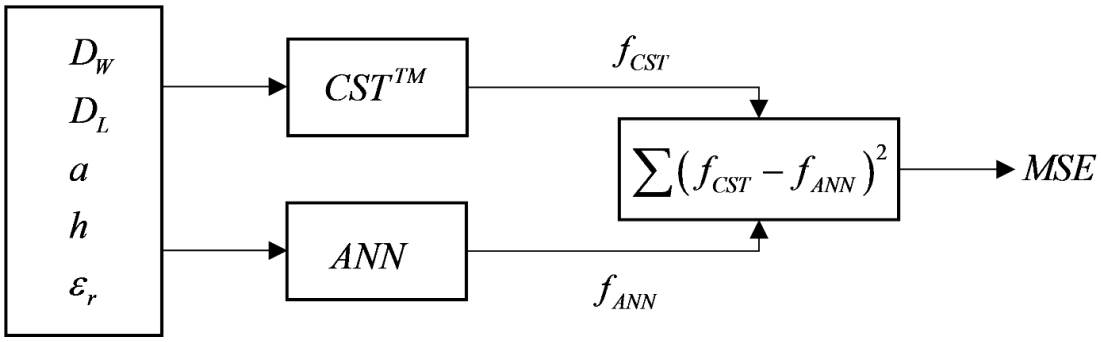

Figure 4. The topology of calculating MSE.

Table 4. Neural Network Tool parameters and values.

Neural Network Tool Dataset	Amount of Data	Percentage of Data
Total Data	144	%100
Training	100	%70
Test	22	%15
Validation	22	%15

Table 5. Neural Network Tool selected algorithm settings.

Neural Network Tool Parameter	Parameter Values
Epochs	1000
Time	Infinity
Goal	0
Minimum Gradient	10-7
Maximum Failure	6
Momentum Update Value	0.001
Momentum Update Decrement	0.1
Momentum Update Increment	10

Table 6. Neural Network Tool dataset division.

Neural Network Tool Settings	Algorithms
Data Division	Random (dividerand)
Training	Levenberg-Marquardt (trainlm)
Performance	Mean Squared Error (mse)
Calculations	MEX

The antenna data distributed for use during the training phase is defined by ANN according to the parameters in Table 6. The hidden layer values and the number of neurons that give sense to the input and output values in the ANN structure should be calculated with different combinations to calculate them with the optimal and most efficient accuracy. This calculation aims to vary the number of layers and neurons according to the variety of data and values they receive in an ANN structure. In other words, with a standard format, it is impossible to capture a large variety of data with ANNs with a low error rate. For this reason, efficiency tests for the parameter's "gain", "directivity", "resonant frequency" and "bandwidth" were performed in this study. The tests were performed in an ANN structure where the number of neurons was'10,20,30,40' and the number of hidden layers was '1,2,3,4'.

During the training phases, the accuracy value of the training results is calculated between 0-1 using the “nntool”. The closer the validation values are to 1, the more efficiently the data is trained, and the more successful the consistency of the data will be. For the ANN architectures determined in the test section, the training stages for the parameters "gain", "directivity", "resonant frequency" and "bandwidth" were completed. When Table 7 is analyzed, four hidden layer structures consisting of 10 neurons have an accuracy rate of 0.9968 for the directivity parameter and an accuracy rate of 0.99654 for the two hidden layer structures consisting of 10 neurons for the gain parameter. In these designs, two hidden layer structures consisting of 10 neurons were conceded with an accuracy rate of 0.99634 for the resonant frequency. Also, the bandwidth parameter determined four hidden layer structures consisting of 10 neurons with an accuracy of 0.99442. It is found that the efficiency is relatively low for structures with a neuron count of "20, 30, 40" and a hidden layer count of "1, 3".

Table 7. NN Tool accuracy ratios on different Neural Network Architectures.

Neural Network Accuracy		Neuron Number			
Hidden Layer Number		10	20	30	40
Directivity	1	0.98255	0.98785	0.97505	0.97667
	2	0.99397	0.98845	0.92796	0.92486
	3	0.98971	0.97535	0.98469	0.93001
	4	0.9968	0.97165	0.97237	0.96334
Gain	1	0.95834	0.98929	0.98818	0.98119
	2	0.99654	0.98987	0.98697	0.99319
	3	0.99231	0.9869	0.99046	0.98903
	4	0.99453	0.98163	0.9871	0.96583
Resonant Freq.	1	0.98824	0.99122	0.99292	0.99206
	2	0.99634	0.98554	0.97075	0.94768
	3	0.99612	0.98419	0.97845	0.93934
	4	0.98039	0.93321	0.98886	0.9772
Bandwidth	1	0.96159	0.94031	0.97575	0.99359
	2	0.99384	0.98509	0.92125	0.91921
	3	0.97319	0.98958	0.9677	0.89707
	4	0.99442	0.95325	0.94078	0.90051

The optimal ANN training steps are performed on an AMD Ryzen™ 7 3700U processor with a base clock speed of 2.3 GHz and AMD Radeon™ RX Vega 10 integrated graphics with 1 GB VRAM and 16 GB DDR4 RAM system.

3. Results and Discussion

3.1. Simulation Results

In this section, the electromagnetic analysis of the proposed monopole patch antenna is performed. The gain curve of the designed antenna for 1.866 GHz is shown in 3-D dimensions. The surface current distribution is shown in Fig. 5. The antenna gain for 1.866 GHz is 2.77 dBi, and the surface current distribution is 26.8 dB(A/m).

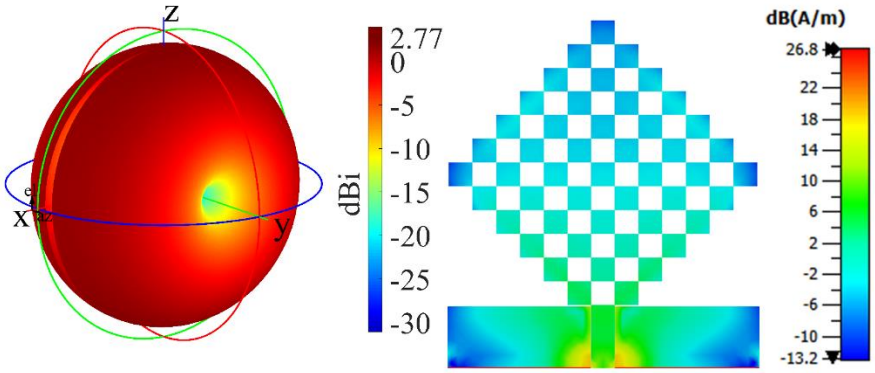

a) b)

Figure 5. a) Antenna 3-D directivity gain, b) Surface current distribution.

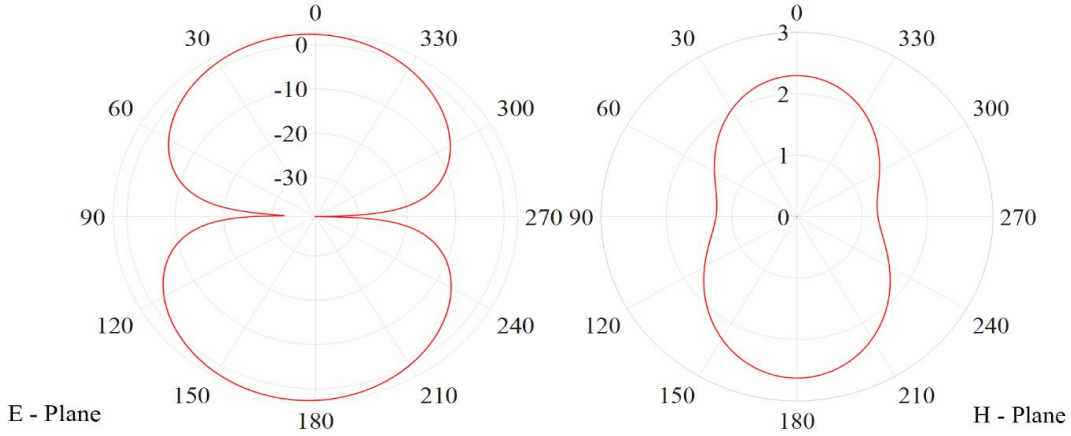

Figure 6. E-plane and H-plane of the Proposed Antenna.

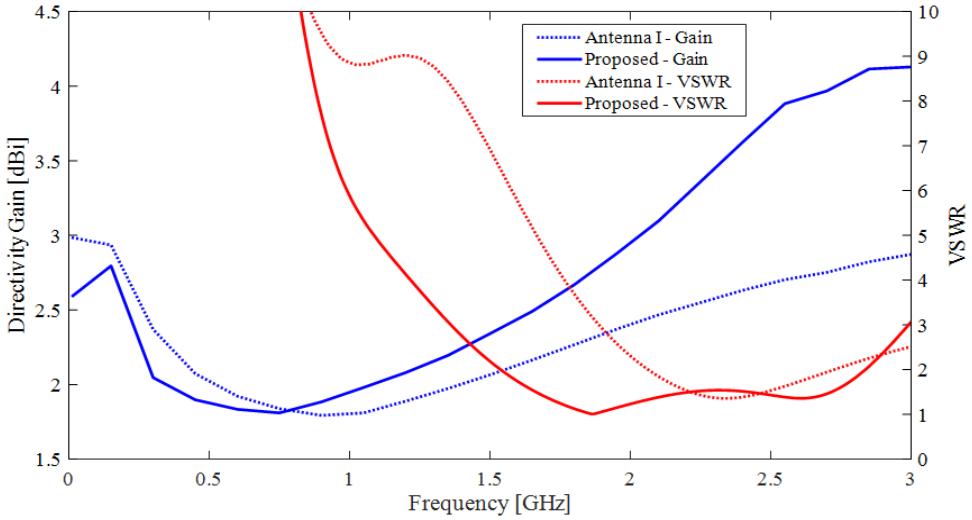

Figure 7. VSWR and Directivity Gain of the Antenna I and Proposed Antenna.

The radiation pattern refers to the directional (angular) shape of the power of the electromagnetic waves radiated by the antenna. Fig. 6. shows the E-plane and H-plane of the proposed antenna.

Fig. 7. shows the voltage standing wave ratio (VSWR) and frequency-dependent gain of Antenna I and the proposed antenna. Proposed antenna operating frequencies 1.55 GHz-2.82 GHz range from 2.39-4.11 dBi.

3.2. Neural Network and Simulation Results Comparison

This section compares simulation and ANN data of 144 consecutive square-shaped monopole patch antennas. Different physical and electrical parameters of the proposed antenna can be calculated with high accuracy for the gain, directivity gain, resonant frequency, and bandwidth parameters determined by ANNs. It can be seen from Fig. 8. and Table 9. that directivity data obtained as a result of the ANN simulation data can predict the NN directivity values with 99.4225% accuracy.

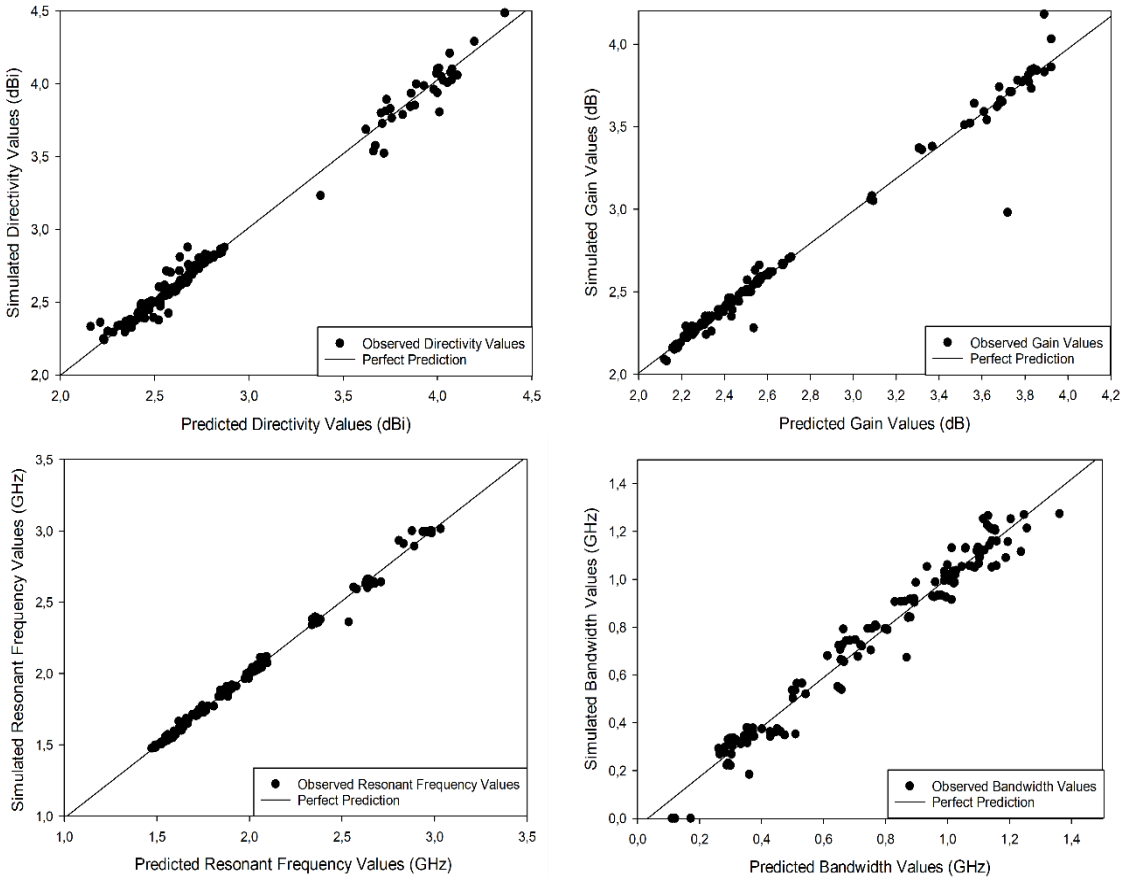

Figure 8. Regression-Based Comparison of CST And NN Data.

Comparing the gain, resonant frequency, and bandwidth with the training results, it is seen that directivity is the parameter with the lowest accuracy among them. Nevertheless, it can be seen that the data from ANN completed the training phases with high accuracy for the directivity parameter and closely approximated the simulation data. Furthermore, an accuracy rate of 99.5237% was calculated for the gain parameter. Although this accuracy rate shows that the gain data is predicted at a very consistent and high rate, it can be seen that the simulation and ANN data are quite close. Additionally, comparing the resonant frequency with gain, directivity, and bandwidth, it is seen that it is the best-predicted parameter which is 99.9097%. It can be observed that the most consistent and highest rate of gain data is estimated for the resonant frequency parameter, for which the highest accuracy rate is calculated. Bandwidth parameter, the average MSE error value of 144 antennas is calculated as 0.00383722. When the bandwidth values are analyzed, prediction accuracy is calculated as 99.6163% by the ANN training. In Table 8. CST™, simulations of 144 consecutive square monopole antennas are compared with the resolution times of the training processes using MATLAB™ "nntool". The comparison of analysis times shows that the analyzed using MATLAB™ "nntool" are 2769.231 times faster than those using CST™.

Table 8. Resolution times comparison of 144 microstrip antennas on CST and NN.

Resolution Time of 144 Microstrip Patch Antennas Analysis with CST™ 3D Electromagnetic Analysis Software	Resolution Time of 144 Microstrip Patch Antennas Analysis with Feed Forward Back Propagation Neural Network On MATLAB™
720 Minutes	0.26 Minutes

As a result of the ANN training, S11 parameters are obtained as predicted ANN. S11 parameters are compared with ANN, CST™, and measurement results in data in Fig. 9. The predicted ANN, simulation using CST™, and measurement results agree. The optimization takes only about 15.6s seconds to achieve the optimal solution for the proposed antenna, as shown in Fig. 9. Minor discrepancies are being detected between the obtained simulation results and the actual measurements. These discrepancies can be attributed to production tolerances, SMA connector characteristics, and losses associated with coaxial cables. However, it is important to note that the observed differences fall within an acceptable range, and the simulation accurately captures the overall trends and characteristics of the antenna. This indicates the successful implementation of the design, with the simulation providing reliable results.

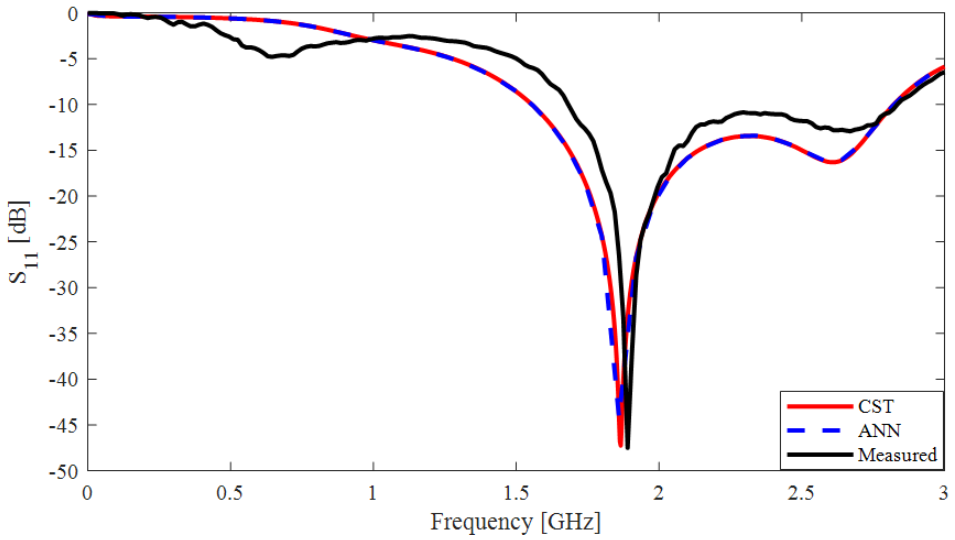

Figure 9. Comparison of S_{11} for CST™ ANN and Measured Antenna.

4. Conclusion

In this study, a new monopole patch antenna design operating at DCS (1.71-1.88 GHz), PCS (1.85-1.99 GHz), UMTS (1.92-2.17 GHz) LTE 2300 (Band-40) 2300-2400 and ISM (IEEE 802.11 b/g/n) 2400-2495 bands is proposed. To increase the return loss of the square antenna in the proposed antenna design, consecutively placed square structures are used in the design. According to simulation and measurement results with electromagnetic analysis software, the directivity gain value varies from 2.16 dBi to 4.18 dBi. However, the proposed antenna has a return loss of -47.25 dB, a gain value ranging from 2.3397 dB to 4.557 dB, and a bandwidth value of 1.27 GHz. In keeping with the simulation data obtained, it was determined that the antenna can provide high return loss and work within the appropriate frequency ranges for wireless communication systems. The proposed consecutive square-shaped monopole antenna, the simulation data, and the generated data for training of ANN model with different geometrical parameters and dielectric constant with the size CST™ 144 antenna was designed, and the simulation process was carried out.

Table 9. Comparison of simulation and ANN data for directivity, gain, resonant frequency, and bandwidth parameters.

	Antenna Number	h	D_L	D_W	a	ε_r	CST Data	NN Data	MSE Error
Directivity	1	0.787	75	65	4	4.3	2.29	2.2813	0.00007500
	7	0.787	75	75	4	4.3	2.16	2.1588	0.00000156
	17	0.787	80	70	4.5	4.3	2.3	2.2902	0.00009616
	25	0.787	85	65	4	4.3	2.29	2.2497	0.00162673
	45	1.575	75	75	5	4.3	2.5	2.4821	0.00031934
	59	1.575	80	80	4,5	4.3	2.34	2.3344	0.00003112
	73	0.787	75	65	4	2.2	2.57	2.5064	0.00404609
	87	0.787	80	65	5	2.2	2.7	2.7956	0.00000001
	92	0.787	80	75	4,5	2.2	2.54	2.5341	0.00003477
	109	1.575	75	65	4	2.2	2.98	3.2318	0.54718650
	132	1.575	80	80	5	2.2	3.65	3.6946	0.00198841
	144	1.575	85	80	5	2.2	3.66	3.6860	0.00067387
Gain	1	0.787	75	65	4	4.3	2.4707	2.5319	0.00374381
	6	0.787	75	70	5	4.3	2.4288	2.4143	0.00021010
	11	0.787	75	80	4.5	4.3	2.292	2.2805	0.00013258
	21	0.787	80	75	5	4.3	2.3918	2.4163	0.00059984
	33	0.787	85	75	5	4.3	2.3943	2.4339	0.00156787
	55	1.575	80	75	4	4.3	2.5916	2.5885	0.00000961
	74	0.787	75	65	4.5	2.2	2.7145	2.6326	0.00670446
	88	0.787	80	70	4	2.2	2.7036	2.5859	0.01384692
	105	0.787	85	75	5	2.2	2.7144	0.6639	0.00000027
	134	1.575	85	65	4.5	2.2	4.101	4.0782	0.00051887
	142	1.575	85	80	4	2.2	4.557	4.2741	0.08005462
	144	1.575	85	80	5	2.2	3.8282	3.7502	0.00608481
Resonant Frequency	5	0.787	75	70	4.5	4.3	1.625	1.6444	0.00037780
	16	0.787	80	70	4	4.3	1.7353	1.7615	0.00068770
	21	0.787	80	75	5	4.3	1.5	1.5071	0.00005111
	29	0.787	85	70	4.5	4.3	1.62	1.6212	0.00000150
	38	1.575	75	65	4.5	4.3	1.918	1.9060	0.00014473
	61	1.575	85	65	4	4.3	2.1116	2.0586	0.00280466
	67	1.575	85	75	4	4.3	2.0648	2.0586	0.00003785
	79	0.787	75	75	4	2.2	2.0428	2.0352	0.00005803
	89	0.787	80	70	4.5	2.2	1.8675	1.8745	0.00004965
	102	0.787	85	70	5	2.2	1.7233	1.7229	0.00000016
	109	1.575	75	65	4	2.2	2.3606	2.5368	0.03105182
	139	1.575	85	75	4	2.2	2.9987	2.9854	0.00017772
Bandwidth	2	0.787	75	65	4.5	4.3	0.3155	0.3542	0.00150084
	11	0.787	75	80	4.5	4.3	0.3284	0.3458	0.00030151
	33	0.787	85	75	5	4.3	0.2923	0.2808	0.00013201
	43	1.575	75	75	4	4.3	0.9836	1.0209	0.00138866
	77	0.787	75	70	4.5	2.2	0.6734	0.8686	0.03811404
	84	0.787	75	80	5	2.2	0.5383	0.6582	0.01436650
	91	0.787	80	75	4	2.2	1.9972	0.3476	0.00000001
	111	1.575	75	65	5	2.2	1.2136	1.2564	0.00182937
	120	1.575	75	80	5	2.2	0.7936	0.7991	0.00003011
	127	1.575	80	75	4	2.2	1.0669	1.1016	0.00120707
	135	1.575	85	65	5	2.2	1.27	1.2476	0.00049971
	142	1.575	85	80	4	2.2	1.0327	0.9899	0.00183038

MSE Error of Directivity For 144 Antennas is 0.00577501	MSE Error of Gain For 144 Antennas is 0.00476269	MSE Error of Resonant Frequency For 144 Antennas is 0.00090232	MSE Error of Bandwidth For 144 Antennas is 0.00383722

Moreover, the results of the Mean Error Squared (MSE) obtained as a result of this training, the directivity values were calculated as 0.00577501 MSE, the gain values as 0.00476269 MSE, the resonant frequency values as 0.00090232 MSE and the bandwidth as 0.00383722 MSE. As a result of the error rates obtained, it has been determined that the most efficient resonant frequency values can be calculated through ANNs. However, resonant frequency, bandwidth, gain, and directivity parameters can be calculated with an accuracy of 99.61805% using ANNs. In addition to the accuracy of the calculations, the Feed Forward Back Propagation Neural Network, designed via MATLAB™ can calculate the data obtained from the CST™ 719.77 minutes faster. The results of this study confirm that simulation data obtained in computer-aided antenna analysis allows researchers to make fast and consistent predictions in analysis, optimization, and measurement studies through ANNs. In the design stages of monopole antennas developed within the scope of increasing data rate, continuity, and security demand in today's wireless communication technologies, ANN can be used effectively by the results obtained in this study.

Authors' Contributions

All authors contributed equally. All authors read and approved the final manuscript.

Competing Interests

The authors declare that they have no competing interests.

References

[1]. A. Nella and A. S. Gandhi, "A survey on microstrip antennas for portable wireless communication system applications," *2017 International Conference on Advances in Computing, Communications and Informatics (ICACCI)*, Udupi, India, 2017, pp. 2156-2165.

[2]. R. S. Daniel, "A CPW-fed rectangular nested loop antenna for Penta band Wireless Applications," *AEU - International Journal of Electronics and Communications*, vol. 139, no. 3, pp. 16-24, 2021.

[3]. S. Ibnyaich, L. Wakrim, and M. M. R. Hassani, "Nonuniform semi-patches for designing an Ultra-wideband PIFA antenna by using genetic algorithm optimization," *Wireless Personal Communications*, vol. 117, no. 2, pp. 957-969, 2020.

[4]. E. A. Aydın, "3D-printed graphene-based bow-tie microstrip antenna design and analysis for Ultra-Wideband Applications," *Polymers*, vol. 13, no. 21, p. 3724-3744, 2021.

[5]. K. L. Chung and C.-H. Wong, "Wang-shaped patch antenna for wireless communications," *IEEE Antennas and Wireless Propagation Letters*, vol. 9, pp. 638-640, 2010.

[6]. K. Sumathi, "Pentagon-shaped MIMO antenna for INSAT C band applications," *Arabian Journal for Science and Engineering*, vol. 47, no. 3, pp. 3611-3618, 2022.

[7]. A. G. Ambekar and A. A. Deshmukh, "E-shape microstrip antenna for dual frequency WLAN application," *Progress In Electromagnetics Research C*, vol. 104, pp. 13-24, 2020.

[8]. A. M. Abdulhussein, A. H. Khidhi, and A. A. Naser, "Omnidirectional microstrip patch antenna for 2.4 GHz wireless communications," *3rd International Conference in Physical Science and Advanced Materials (PAM 2021)*, Istanbul, Turkey, 2021, pp. 012051.

[9]. L. Lizzi, R. Azaro, G. Oliveri, and A. Massa, "Printed UWB antenna operating over multiple mobile wireless standards," *IEEE Antennas and Wireless Propagation Letters*, vol. 10, pp. 1429-1432, 2011.

[10]. K. Yadav, A. Jain, N. M. Osman Sid Ahmed, S. A. Saad Hamad, G. Dhiman, and S. D. Alotaibi, "Internet of thing-based Koch fractal curve fractal antennas for wireless applications," *IETE Journal of Research*, pp. 1-10, 2022.

[11]. O. Benkhadda, M. Saih, K. Chaji, S. Ahmad, and A. Reha, "A compact dual-band CPW-fed slot monopole antenna for WIFI, WLAN and WiMAX applications," *Arabian Journal for Science and Engineering*, 2022.
[12]. H. Alam and M. Y. Jamal, "A novel modified T slot to realize wideband circularly polarized patch antenna for low-cost planar 2.4 ghz wireless LAN, Bluetooth, GPS applications," *IETE Journal of Research*, pp. 1-6, 2021.
[13]. R. Azim, M. T. Islam, and N. Misran, "Microstrip line-fed printed planar monopole antenna for UWB applications," *Arabian Journal for Science and Engineering*, vol. 38, no. 9, pp. 2415-2422, 2013.
[14]. D. Rishishwar and L. Shrivastava "Rectangular microstrip patch antenna with FSS and slotted patch to enhance bandwidth at 2.4 GHz for WLAN applications," *International Journal of Technology Enhancements and Emerging Engineering Research (IJTEEE)*, vol. 2, no. 4, pp. 59-62, 2014.
[15]. Z. A. Nassr, S. N. Zabri, N. A. Shairi, Z. Zakaria, A. Othman, and A. M. Zobilah, "Performance improvement of a slotted square patch antenna using FSS superstrate for wireless application," *International Conference on Telecommunication, Electronic and Computer Engineering*, Melaka, Malaysia, 2019, p. 012030.
[16]. T. D. Amalraj and R. Savarimuthu, "Design and analysis of microstrip patch antenna using periodic EBG structure for C-band applications," *Wireless Personal Communications*, vol. 109, no. 3, pp. 2077-2094, 2019.
[17]. R. Biswas, A. Nandi, M. K. Parsha, and B. Basu, "High isolation, wide aperture antenna array using auxiliary feeds and EBG surface for 5G communication," *Arabian Journal for Science and Engineering*, vol. 47, no. 11, pp. 14935-14945, 2022.
[18]. I. Catalkaya, "A Broadband High Gain Antenna with Parasitic Elements for Wireless Applications", *Journal of Aeronautics and Space Technologies (JAST)*, vol. 13, no. 1, pp. 121-128, 2020.
[19]. S. Rekha and S. R. Jino Ramson, "Parasitically isolated 4-element MIMO antenna for 5G/WLAN applications," *Arabian Journal for Science and Engineering*, vol. 47, no. 11, pp. 14711-14720, 2022.
[20]. K. W. S. Al Kharusi, N. Ramli, S. Khan, M. T. Ali, M. A. Halim "Gain enhancement of rectangular microstrip patch antenna using air gap at 2.4 GHz." *International Journal of Nanoelectronics and Materials*, vol. 13, no.19, pp. 211-224, 2020.
[21]. D. Uzer and S. S. Gultekin, "An investigation of shorting pin effects on circular disc microstrip antennas," *International Journal of Applied Mathematics, Electronics and Computers*, vol. 3, no. 3, p. 218, 2015.
[22]. X. Yang, L. Ge, J. Wang, and C.-Y.-D. Sim, "A differentially driven dual-polarized high-gain stacked patch antenna," *IEEE Antennas and Wireless Propagation Letters*, vol. 17, no. 7, pp. 1181–1185, 2018.
[23]. Y. A. Sheikh, K. N. Paracha, S. Ahmad, A. R. Bhatti, A. D. Butt, and S. K. Rahim, "Analysis of compact dual-band Metamaterial-based patch antenna design for Wearable Application," *Arabian Journal for Science and Engineering*, vol. 47, no. 3, pp. 3509-3518, 2021.
[24]. A. Bakhtiari, R. A. Sadeghzadeh, and M. N. Moghadasi, "Gain enhanced miniaturized microstrip patch antenna using metamaterial Superstrates," *IETE Journal of Research*, vol. 65, no. 5, pp. 635-640, 2018.
[25]. L. Lizzi, F. Viani, E. Zeni, and A. Massa, "A DVBH/GSM/UMTS planar antenna for multimode wireless devices," *IEEE Antennas and Wireless Propagation Letters*, vol. 8, pp. 568-571, 2009.
[26]. J. Row and Y. Liou, "Broadband short-circuited triangular patch antenna," *IEEE Transactions on Antennas and Propagation*, vol. 54, no. 7, pp. 2137-2141, 2006.
[27]. C. H. See, R. A. Abd-Alhameed, D. Zhou, T. H. Lee, and P. S. Excell, "A crescent-shaped multiband planar monopole antenna for mobile wireless applications," *IEEE Antennas and Wireless Propagation Letters*, vol. 9, pp. 152-155, 2010.

[28]. B. Wang, F. Zhang, T. Li, Q. Li and J. Ren, "A novel wideband circular patch antenna for wireless communication," *2014 International Symposium on Antennas and Propagation Conference Proceedings*, Kaohsiung, Taiwan, 2014, pp. 545-546.

[29]. M. Aneesh, A. Singh, K. Kamakshi, and J. A. Ansari, "Performance investigations of S-shaped RMSA using multilayer perceptron neural network for S-band applications," *Radioelectronics and Communications Systems*, vol. 62, no. 8, pp. 400-408, 2019.

[30]. P. K. Abbassi, N. M. Badra, A. M. M. A. Allam and A. El-Rafei, "WiFi Antenna Design and Modeling using Artificial Neural Networks," *2019 International Conference on Innovative Trends in Computer Engineering (ITCE)*, Aswan, Egypt, 2019, pp. 270-274.

[31]. M. Sagik, O. Altintas, E. Unal, E. Ozdemir, M. Demirci, S. Colak, and M. Karaaslan, "Optimizing the gain and directivity of a microstrip antenna with metamaterial structures by using artificial neural network approach," *Wireless Personal Communications*, vol. 118, no. 1, pp. 109-124, 2021.

[32]. A. Kayabasi, A. Toktas, A. Akdagli, M. B. Bicer, D. Ustun "Applications of ANN and ANFIS to predict the resonant frequency of L-shaped compact microstrip antennas," *The Applied Computational Electromagnetics Society Journal (ACES)*, vol. 29, no. 6, pp. 460-469, 2021.

[33] Z. Yang, Y. Zhang, L. Zhu, L. Huang, F. Hu, Y. Du and X. Li, "MSCNN-LSTM model for predicting return loss of the UHF antenna in HF-UHF RFID tag antenna" *Computers, Materials & Continua*, vol. 75, no. 2, pp. 2889-2904, 2023.

[34] R. Karanam and D. Kahkar, "Artificial neural network optimized ultra-wide band fractal antenna for vehicular communication applications." *Transactions on Emerging Telecommunications Technologies*, vol. 33, no. 12, 2022.

[35] D. Sami Khafaga, A. Ali Alhussan, E.-S. M. El-kenawy, A. Ibrahim, S. H. Abd Elkhalik, S. Y. El-Mashad and A. A. Abdelhamid, "Improved prediction of metamaterial antenna bandwidth using adaptive optimization of LSTM," *Computers, Materials & Continua*, vol. 73, no. 1, pp. 865-881, 2022.